Ciências da Terra (UNL)	Lisboa	Nº 17	pp. 29-44, 11 fig.	2010

Orbital forcing of stratal patterns in an inner platform carbonate succession: an example from an Upper Hauterivian series of the Lusitanian Basin, Portugal

Carine Lezin[1, 2], Louis Bonnet[1], Jacques Rey[1], Paulo S. Caetano[3], Paula Gonçalves[4], Fernando Rocha[4] & Rogério B. Rocha[3]

[1] Université de Toulouse; UPS – CNRS - IRD; Laboratoire des mécanismes de transfert en Géologie (OMP), 14 av. Edouard Belin, F-31400 Toulouse, France; carine.lezin@lmtg.obs-mip.fr, jacques.rey3@free.fr
[2] UMR-CNRS 5563 & IRD, LMTG, F 31400 Toulouse, France
[3] CICEGe, Universidade Nova de Lisboa, Faculdade de Ciências e Tecnologia, Campus de Caparica, 2829-516 Caparica, Portugal; pcsc@fct.unl.pt, rbr@fct.unl.pt
[4] GEOBIOTEC, Departamento de Geociências, Universidade de Aveiro, Campus de Santiago, 3810-193 Aveiro, Portugal; paulac.goncalves@gmail.com, tavares.rocha@ua.pt

Resumo

Palavras-chave: Variações estratonómicas, ambientes de plataforma interna, ciclos orbitais, Hauteriviano, Portugal

Através de exemplo retirado de uma série tardi-hauteriviana da Bacia Lusitaniana (Portugal), é demonstrado o registo sedimentar de variações de padrões orbitais e, consequentemente, de variações climáticas num ambiente de plataforma interna com sedimentação agradante contínua.

A comparação de variações de espessuras de camadas, que reflectem taxas de produção carbonatada, com a variação de padrões orbitais combinadas com modificações de insolação, permite distinguir quatro principais ordens de periodicidade relacionadas com componentes orbitais:

- Grandes ciclos de variação de espessuras, constituídos por 31-32 camadas, que registam a componente do ciclo de excentricidade de 400 ky;
- Ciclos médios, representados por pacotes de 8-9 camadas, relacionados com a componente do ciclo de excentricidade de 100 ky;
- Ciclos pequenos, de 3-5 camadas, que registam a componente de obliquidade de 41 ky;
- Ciclos muito pequenos, de 2 camadas, relacionados com as componentes de precessão de 22 ky e de 26 ky.

A duração média calculada para cada estrato é de cerca de 11,8 ky, um valor muito próximo do correspondente ao semi-ciclo de precessão.

Também é demonstrado que as variações na micritização são igualmente correlacionadas com variações estratonómicas e orbitais.

Abstract

Key-words: Stratal variations, inner platform environments, orbital cycles, Hauterivian, Portugal

With an example taken from a late-Hauterivian series of the Lusitanian Basin (Portugal), we will demonstrate the sedimentary record of orbital pattern variations and, consequently, climate variations in an inner platform environment with continuous aggrading sedimentation.

The comparison of the variation of bed thicknesses, which reflects carbonate production rates, with that of combined orbital patterns and insolation changes, allows us to establish 4 major orders of periodicity related to orbital components:

– The large cycles of bed thickness variation, constituted by 31-32 beds, recording the 400 ky eccentricity cycle component;
– The medium cycles, represented by bundles of 8-9 beds, related to the 100 ky eccentricity cycle component;
– The small cycles, of 3-5 beds, recording the 41 ky obliquity components;
– The very small cycles, of 2 beds, related to the 22 ky and 26 Ky precession components.

The mean duration of each bed is around 11.8 ky, a number very close to that of the precession hemi-cycle.

Climatic control on quantitative and qualitative carbonate production is confirmed by the close relation between the bed thickness variations, the insolation variability and the variation of micritized elements concentrations.

1. Introduction

Carbonate production resulting exclusively from biological activity is controlled by retroactive factors, both internal and external to the sedimentary environment. The production fluctuations are expressed by facies and lithological changes and/or by variations of the quantity of carbonate produced per unit of time.

It has been shown, in pelagic environments, that variations of the carbonate production rate are expressed by thickness variations of the carbonated beds (Kennett, 1982).

Fischer & Schwarzacher (1984) showed, in Barremian and Cenomanian pelagic series of alternating carbonate-rich marly beds in Italy (Maiolica and Scalia Bianca), a periodicity in the thicknesses frequencies of the limestone deposits corresponding to the orbital periods of 100 Ky, 41 Ky and 19-23 Ky. Foucault & Renard (1987) observed a narrow parallelism between the frequency curve of bed thicknesses and the $\delta^{18}O$ fluctuations of total carbonate, which also confirms the climatic control of pelagic carbonate sedimentation.

Thus the following question may be put: if climatic variations control carbonate production in basinal areas, can the same occur in platform areas, in spite of the number of implied producers being more important and the factors controlling carbonate production being more numerous?

Few studies have attempted to analyse the way in which climate changes are recorded in platform environments with very contrasting sedimentation. They show a relation between facies or sedimentation rate changes and orbital pattern variations (e. g. D'Argenio *et al.*, 1997; Strasser *et al.*, 1999; Yang & Lehrmann, 2003). Insufficient dating, variable sedimentation rates, discontinuous sedimentation, and hiatuses (erosion, emersion) may complicate their recognition.

The main objective of this paper is to describe periodic structures that have been observed in an inner platform, relatively little contrasted, carbonate series, and which can be related to Milankovitch cycles. It deals with an Upper Hauterivian succession in the Lusitanian Basin in Portugal, deposited in a subtidal inner platform environment.

2. Geographical and geological framework

The Lusitanian Basin, near the Iberian continental margin, is an intra-cratonic basin showing a generally weak but irregular subsidence during the Cretaceous (approximately 700 m maximum thickness of non-decompacted sediments for 53 My). During the Lower Cretaceous sedimentation was of fluvial character over most of the basin. In the Lisbon region marine conditions dominated (fig. 1) with a surrounding up to 10 km wide siliciclastic coastal plain and a sub-tidal platform with dominantly carbonate sedimentation (Rey, 1972). The depocentre is found in the vicinity of the town of Cascais.

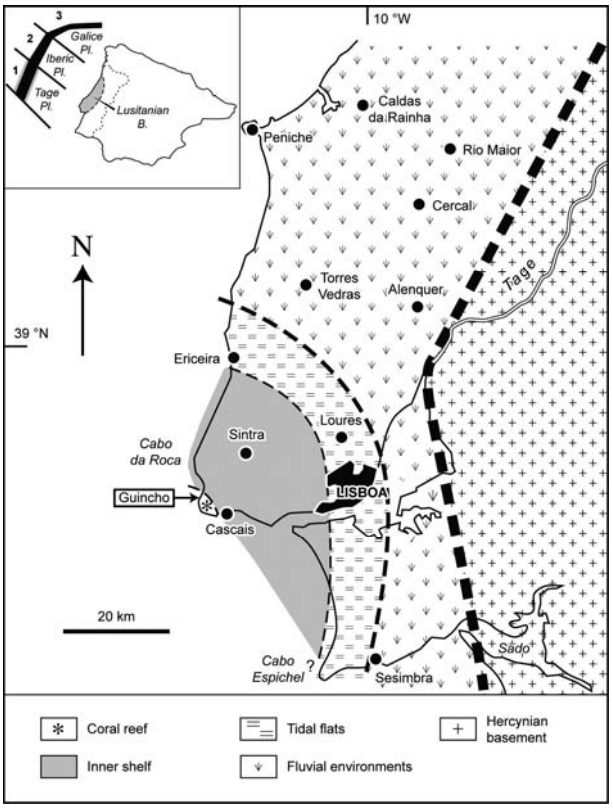

Fig. 1 – Geographical location and geological framework.

During the Lower Cretaceous, the Lusitanian Basin was strongly influenced by the different Atlantic opening episodes along the Iberian plate. Thus the entire succession is organised into three transgressive-regressive 2nd order cycles, separated by intervals produced by events that seem to coincide with the major oceanic accretion propagation stages (Rey *et al.*, 2003):

- A Valanginian – Upper Barremian cycle, following the neo-Cimmerian event, which would be contemporary to the beginning of the oceanic accretion North of the Azores fracture lineament, in particular in the Tagus sector (fig. 1);
- An Upper Barremian – Lower Aptian cycle, following the intra-Barremian event, which would be associated to the appearance of the first oceanic crust in the Iberian sector (fig. 1);
- An Upper Aptian *pro parte* – Albian cycle, separated from the former by the «Austrian» event, which would be related to the appearance of the first oceanic crust in the Galicia sector (fig. 1).

The sedimentary succession for the Upper Valanginian – Albian is organized in to thirty-seven 3rd order depositional sequences (Rey *et al.*, 2003) that express sea-level variations whose origin, climatic and/or tectonic, remains to be fully demonstrated.

2.1. *The Late-Hauterivian series*

The studied section outcrops along the cliffs North of Praia Grande do Guincho, 30 km to the West of Lisbon and 7.5 Km to the North-West of Cascais (fig. 1). It is formed by a 45 m thick succession of limestone beds intercalated with argillaceous limestones and occasional marly beds.

It is composed of a succession of perfectly tabular beds in which no sedimentary structures are visible. The biophase (fig. 2) is composed exclusively of gastropods (Nerinae, Naticid and *Ptygmatis* sp.), lamellibranchiata (ostreids), abundant and diversified benthic Foraminifera, algae and remains of echinodermata, corals, rudists, *Bacinella irregularis* and *Lithocodium aggregatum*. Among the calcareous algae, the dasycladals prevail, in particular, the genus *Terquemella*, *Salpingoporella*, *Cylindroporella* and *Pseudoactinoporella*.

Concerning benthic foraminifera associations, foraminifera with agglutinant test, with simple and complex structure, are the most abundant in the majority of the levels, the species *Choffatella decipiens* being largely represented. The miliolids (genus *Quinqueloculina*, *Pyrgo*, *Pseudotriloculina* and *Istriloculina*) increase their concentration while going upwards in the series. Some foraminifera with hyaline test (genus *Lenticulina*, *Trocholina* and *Neotrocholina*) constitute, in certain levels, the remainder of the biophase.

Micritization is very frequent in this series; it affects all types of bioclasts and induces the presence of abundant pelletoids.

The quantitative analysis of facies parameters together with field observations has allowed the establishment of 6 distinct facies:

1 – Grainstones with badly calibrated debris of corals, rudists and lithoclasts. This facies characterizes high energy environments with allochtonous fossils;

2 – More or less marly limestones (wackstone to wackstone-packstone) with predominance of *Choffatella decipiens*, naticids, *Permocalculus* sp. and locally abundant echinoid debris;

3 – Oncoidal limestones associating *Choffatella decipiens*, other large foraminifera with agglutinated tests, miliolids, textulariids, dasycladals;

4 – Pelletoidal and oncoidal limestones composed exclusively of textulariids, miliolids and dasycladals;

5 – Grainstones with proliferation of miliolids and *Ptygmatis* sp. associated with some textulariids, *Valvulineria* sp., *Arenobulimina* sp. and *Belorussiella* sp.;

6 – Mudstones with rare miliolids (*Istriloculina* sp. and *Pseudotriloculina* sp.) and bioclasts filled by internal sediment.

The biophase (fig. 2) which composes these various facies (dasyclads, milliolids, Foraminifera with agglutinant tests and with complex structures) is characteristic of the subtidal stage in the inner platform (Rey & Cugny, 1977; Arnaud-Vanneau, 1980; Arnaud-Vanneau & Darsac, 1984; Cugny, 1988). The presence of dissolved bioclasts filled by internal sediment in two levels (8 and 76; fig. 3), suggests episodic emersion within the intertidal (bed 76) to supratidal (facies 6, beds 8 and 9) stages.

The absence of sedimentary structures and the presence of carbonate mud in the majority of the levels, attest to very moderate or weak hydrodynamic conditions. These palaeoenvironments and hydrodynamic conditions are also confirmed by the abundance of micritized elements suggesting shallow clear water conditions with weak hydrodynamics (Purser, 1980).

The term “restricted platform” is not appropriate to this case, on the one hand, due to the presence of nodosariids (*Lenticulina* sp.; fig. 2) that suggest open communication with the outer realm and, on the other hand, due to the abundance and diversity of benthic foraminifera and dasycladals that are indication of normal oxygenation and salinity conditions (Flügel, 2004).

2.2. *Sequential interpretation and biochronological data*

The first sequential interpretation of the Lower Cretaceous in the Lusitanian Basin was proposed by Rey *et al.* (2003) based on the study of paleoenvironmental evolution, sedimentary discontinuities, basin scale correlations and on the deposit geometries. Seven 3rd order depositional sequences were recognized in the Hauterivian stage. According to Gradstein *et al.* (2005), this stage covers 6.4 My suggesting an average duration of each Hauterivian sequence of 914 ky.

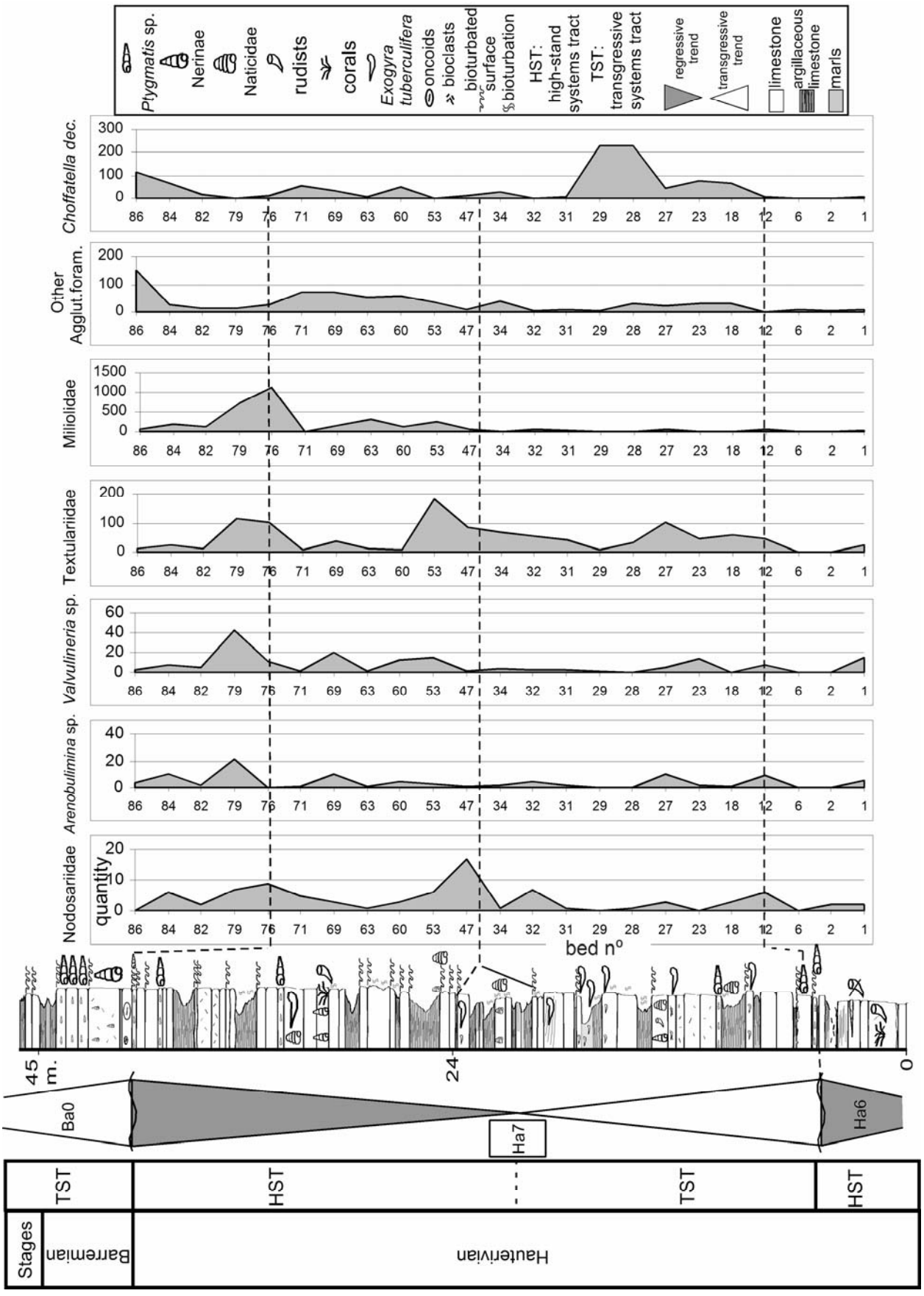

Fig. 2 – Facies variations, distribution of main benthic organisms and sequential interpretation.

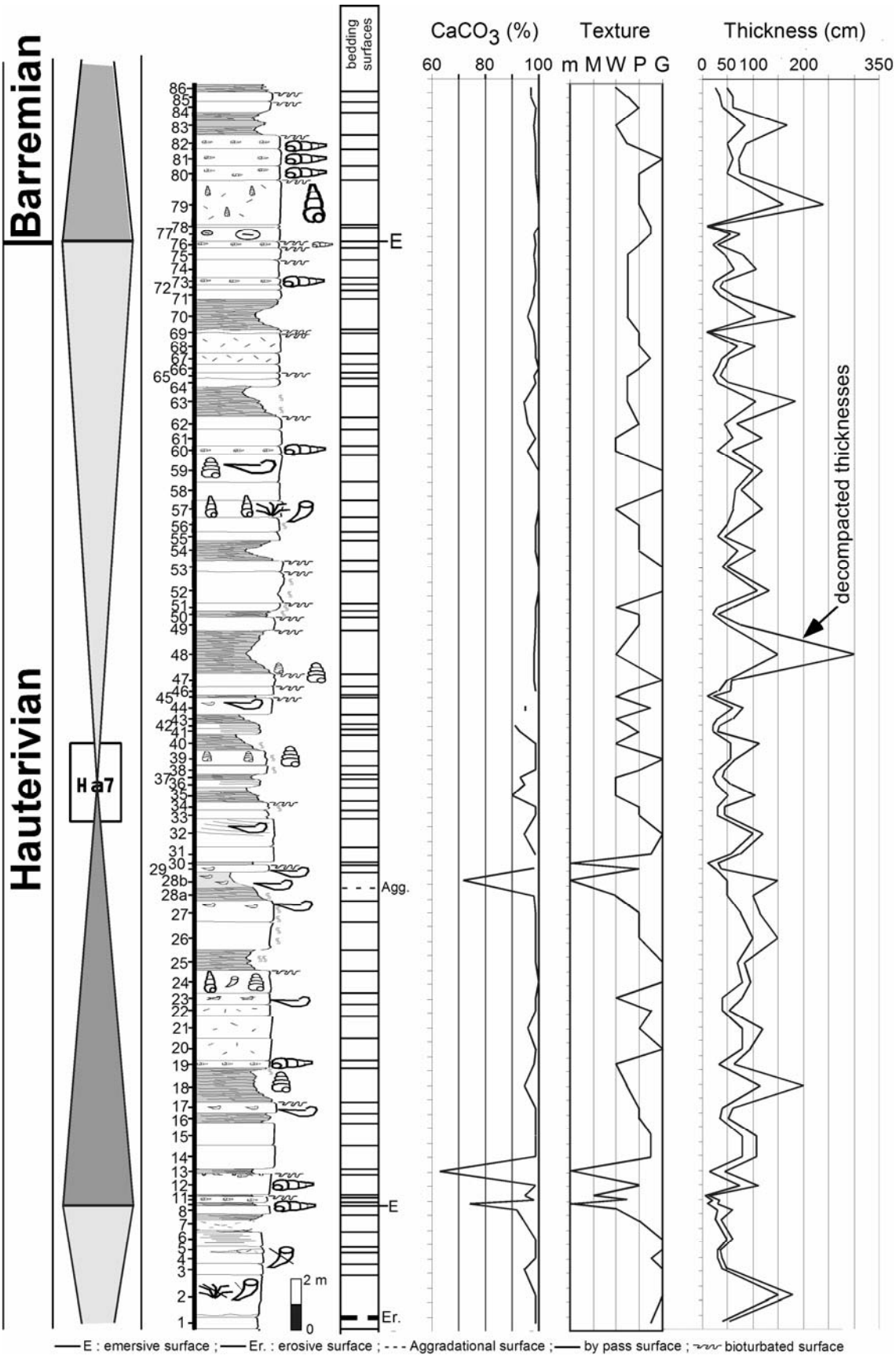

Fig. 3 – Stratal, lithological and textural characteristics.
m: marls; **M**: mudstone; **W**: wackestone; **P**: packstone; **G**: grainstone.

The studied series pertains (fig. 2), in its greater part, to the Ha7 sequence (Rey *et al.*, 2003), but ranges from the summit part of the underlying Ha6 sequence, to the basal part of the overlying Ba0 sequence. This stratigraphic attribution is proved by the presence of the species *Campanuella capuensis* in level 31 and by the identification (Rey, 1972), in the overlying sequence, of *Heteraster couloni* – index species of the Barremian (Villier, 2001).

According to the Hardenbol *et al.* (1998) chart, the base of the Ba0 sequence (level 76) is placed at the Hauterivian- Barremian boundary, dated by Gradstein *et al.* (2005) of -130 ± 1,5 My.

The detailed (bed by bed) faciologic analysis of this succession enabled a precise positioning of the various sequence boundaries and systems tracts, which are difficult to apprehend by a simple field survey.

This series shows the following characteristics: the base is made up of grainstones with lithoclast accumulations (corals, rudist remains) which are interpreted as being reef dismantling deposits in high sea level context. These subtidal to intertidal facies pass gradually, while going up in the series, to supratidal facies. The sequence boundary (Ha7) is positioned at the top of bed nº 8 (fig. 3) due to the presence of emersion characteristics.

Subtidal facies very quickly overlay this emersion surface, thus testifying a deepening of the environment (TST, Ha7; fig. 2). The Ha7 lowstand system tract (LST) is missing at the Guincho section.

Above the sequence boundary, the quantitative analysis of benthic foraminifera shows that the 3rd order sequence can be subdivided in 2 large sets:

- A lower part where *Choffatella* sp. predominates;
- An upper part where miliolids progressively increase.

The boundary between these two sets (fig.2) is marked by enrichment in oysters (*Exogyra tuberculifera*), in fine clastics (predominance of argillaceous limestone beds in relation to limestone beds), in *Trocholina* sp., *Neotrocholina* sp. and in nodosariids (*Lenticulina* sp.).

On the other hand, at both ends of the sequence, one can observe the presence of *Ptygmatis* sp. that reveals inter- to supratidal environments (Zhang *et al.*, 2002). In the same way, countings indicate a progressive fall in the concentration in *Valvulineria* sp. from the base to the middle of the sequence. This tendency is then reversed as the boundary with the overlying Ba0 sequence is approached. However, several studies (Arnaud-Vanneau, 1980; Arnaud-Vanneau & Darsac, 1984) show that *Valvulineria* sp. proliferate in lagoonal environments. These arguments point out to the position of the maximum flooding surface around bed nº 36.

Finally, the presence of emersion characteristics expressed by early dissolution of bioclasts and early filling by internal sediment (bed 76), the predominance of gastropods typical of inter- to supratidal environments (*Ptygmatis* sp.), and the very strong enrichment in miliolids – with the presence, in particular, of *Istriloculina* sp., *Pseudotriloculina* sp. – and in *Valvulineria* sp., proving proximity of coastal flats, allows the positioning of the sequence boundary at the top of bed nº 76.

Compared to the other Lower Cretaceous sequences of the Lusitanian Basin, this Ha7 sequence is characterised by an exceptional thickness (2.6 times larger than the average sequence thickness), by relative facies uniformity and by presenting aggrading depositional characteristics.

3. Methods

The methods used to allow the identification of the major parameters which controlled sedimentation within this sequence, were the following:

- Establishing the $CaCO_3$ content (fig. 3), in each bed, by calcimetry.
- Definition of bedding surfaces (fig. 3). These surfaces were described in the field and some were analyzed by optical microscopy. It was possible to distinguish: *aggradational surfaces*, which express a progressive change of lithology or facies without probable nondeposition; *perfectly flat surfaces (bypass surfaces)*, occasionally bioturbated, which testify nondeposition; *erosional surfaces* and *emersion surfaces* (fig. 3). The analysis of these surfaces therefore provides information on the continuous or discontinuous character of sedimentation.
- Decompaction of the studied series (fig. 3). To estimate the variations of sedimentation rate, it was necessary to decompact the series. Within a carbonate series, the lithological variations are generally numerous and texture presents a strong variability (from mudstone to grainstone). For these reasons, the series was decompacted bed by bed, by taking into account these two parameters (lithology and texture). The decompaction factors, used in this study and published by Hillgärtner & Strasser (2003), lie between 1.2 for pure carbonate sand, 2.5 for pure carbonate mud, and 3.0 for marls.
- Statistical data processing. The periodicity test of Johnson (Johnson, 1972), the calculation of the autocorrelation coefficient and the spectral analysis (Chatfield, 1975) were used in order to detect a possible cyclic structure and to define its periodicity.

The variability of the series is computed by means of a moving relative variation coefficient (ratio: standard-deviation/average) with a bed window. The numerical derivative was calculated with the aim of specifying the speed and the direction of variation of the studied parameter.

- Calculation of the orbital series and insolation curve. In order to highlight a possible climatic control on sedimentation, a simulation of the various orbital cycles was carried out by means of software written by one of us and from the data of Berger (1978), between –132 and –128 My in order to widely frame the duration of the section.

The insolation curve was calculated from the following equation:

$$Q = (E_8/\pi)\,[1\text{-}0.25\,\sin^2 B - \sin^2\gamma\,(1\text{-}0.25\,\sin^2 B\text{-}\sin B) + \sin B \sin\gamma - (4/\pi)\,e\,\sin L\cos\gamma]$$

In which: Q = Energy received by the Earth in 6 summer months; E_8 = Constant solar = 1367 watts/m^2 in 6 months; B = Obliquity; E = Eccentricity; L = position of the perihelion compared to the vernal point; γ = latitude.

This formula is quoted in Hufty (2001) and Tricot & Berger (1988). Equivalent calculations appear in the following sites (by Laskar *et al.*): www.Imcce.fr/Equipes/ASD/insola/earth/La2004/insola.f and www.Imcce.fr/Equipes/ASD/insola/earth/La2004/insolsub.f. Moreover, the curve obtained is similar to the curve that can be obtained from the following Internet site: http://www.geo.ed.ac.uk/~jgc/sunshine.html#Applet1

4. Results

4.1. *Stratal variations*

Characteristics of the stratonomic series

The sedimentary sequence includes 87 beds bounded, on both sides, by flat surfaces, sometimes bioturbated (fig. 3). The absence of erosion criteria (except at the top of bed 1) and the localization of bioturbation beneath and above bedding surfaces, lends them a quite particular significance; they testify nondeposition in an immersion context, except at the base and at the top of the sequence (top of beds 8 and 76). Nevertheless, in these two cases, morphology does not change, and no emersion criterion is observed in the field.

Only one bedding surface (between the beds 28a and 28b) corresponds to an aggradational surface testifying a change of lithology without nondeposition.

Thus bedding surfaces correspond to periods of nondeposition of which the duration is difficult to estimate. Nevertheless, being given the strongly similar morphological characteristics, it is probable that the same phenomenon is at the origin of all these nondeposition events. These events are probably related to changes of the paleo-environmental conditions controlled by allocyclic factors.

Therefore, at the scale of the whole series, it can be said that the sedimentary record is discontinuous, as in all environments; however, within each bed the record is continuous (at least on a geological time scale). If it is admitted that the phenomenon at the origin of the nondeposition events has a constant periodicity, it can be considered that each bed corresponds to a unit of time (basic postulate in all cyclostratigraphic studies, in particular in pelagic series). The variations of bed thicknesses would thus reflect variations of sedimentation rate per unit of time.

The variation of the $CaCO_3$ content enables us to specify the type of sedimentation which prevails in this inner platform context. The average carbonate rate is about 96.9 %, and 89.3 % of the beds have a rate equal to, or higher, than 95 %. Only 3 beds contain a significant insoluble fraction. It seems thus obvious that sedimentation is controlled by the carbonate self-production.

Finally the textural analysis, associated to the quantification of the $CaCO_3$ rate, has allowed the decompaction of the series. The comparison of the apparent thicknesses curves (compacted) with the decompacted thicknesses curves shows that there are no obvious modifications of the structure of the variation curve but only of the amplitude (fig. 3).

Periodicity of bed thicknesses

The analysis of the temporal evolution of bed thickness (fig. 4) shows a cyclic structure with the following components:

– *Large cycles* (LC superbundles) comprising two incomplete LC's and two complete ones:

Large cycles (LC)	Boundaries (bed n°)	Comments
LC IV	77 - ?	beginning of a cycle
LC III	46 – 76	complete cycle
LC II	12 - 45	complete cycle
LC I	11	end of a cycle

The calculation of the autocorrelation coefficient between beds 11 and 78 justifies the cyclicity and specifies its periodicity:

Lag	Correlation coefficient: r	Degrees of freedom	Probability
30 beds	0.355	55	0.66%
31 beds	0.577	54	< 0.01 %
32 beds	0.476	53	0.02 %
33 beds	0.450	52	0.06 %
34 beds	0.426	51	0.15 %
35 beds	0.489	50	0.02 %
36 beds	0.278	49	4.55 %

We can conclude that, on average, an interval close to 31 –32 beds separates strongly correlated sets, which confirms the periodicity test of Johnson (Johnson, 1972).

Each large cycle (fig.4) is subdivided into:

– *Medium cycles* (MC bundles), in a number of 4, and each one including 8 or 9 beds. The first 3 MC have important or medium maximum thicknesses of decreasing amplitude. The last one (MC 4), comprises a small maximum thickness framed between two minimums, constitutes the overall minimum of the LC and precedes the following one. The MC's are themselves subdivided into:

– *Small cycles* (SC), in a number of 2 or 3 for each MC, and each comprising 4 or 5 beds. In some SC, another subdivision can be seen:

– *Very small cycles* (VSC), in a number of 2 for each SC, detectable only in the raw data series (beds 11 - 16, 17- 22, 25 - 30, 53 - 62, 72 - 78) and formed by 2 or 3 beds.

In short, the section presents a cyclic structure with 4 different periodicities (fig. 4). If one arbitrarily sets the beginning of a cycle immediately after a minimum thickness, the following boundaries can be proposed for the LC's and the MC's:

Large cycles (LC)	Medium cycles (MC)	Boundaries (bed nº)
LC III - LC IV		bed 77 or 78
	MC 3 - MC 4	bed 72 or 73
	MC 2 - MC 3	bed 65 or 66
	MC 1 - MC 2	between beds 55 and 56
LC II - LC III		bed 45 or 46
	MC 3 - MC 4	bed 37
	MC 2 - MC 3	bed 30
	MC 1 - MC 2	bed 23
LC I - LC II		bed 11 or 13

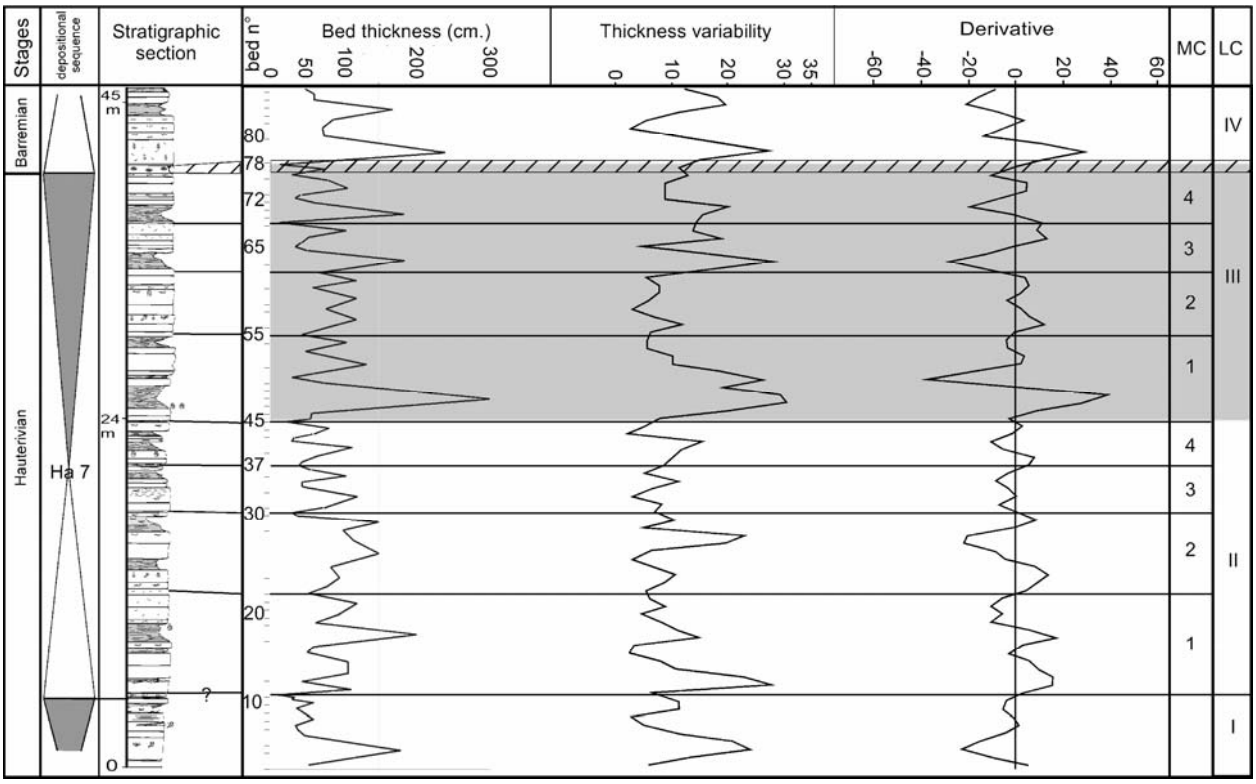

Fig. 4 – Variation of raw data thickness, variability of thicknesses and numerical derivative.

Morphology of the cycles

A large cycle (LC) starts with an abrupt increase of thicknesses. For example, in LC III (fig. 5), thickness values can increase, in only 4 beds (45-48), from 20 to 300 cm, that is to say, an average 93.3 cm for each interval. The regression equation of y (thickness) in x (bed number) shows a very strong positive value of the slope:

$$y = 84.16x - 102.00$$

After the maximum of LC III (bed 48, thickness 300 cm), thicknesses decrease irregularly up until bed 78 (thickness 13.5 cm), with an average rate of 9.6 cm per bed. This decreasing phase, that spreads over 30 beds, is much longer than the increasing phase. The regression equation indicates a weak negative value of the slope:

$$y = -2.06x + 115.38$$

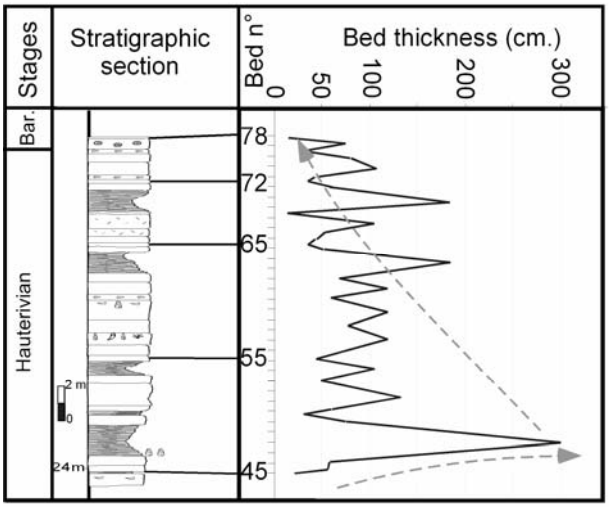

Fig. 5 – Morphology of the large cycle III.

General tendency in the bed thickness series

For the whole of the section, the regression equation of y (thickness) in x (bed number, compared to time) is:

$$y = -0.13x + 84.61$$

The slope of the regression straight line does not differ significantly from 0 (test on the slope: probability = 56.00 %; correlation coefficient: r = 0.063). There is thus no general linear trend in the thicknesses for the whole of the series (fig .3).

Rate of variation and variability of bed thicknesses

The numerical derivative (fig. 4) shows that the speed of thickness increase is large at the beginning of the medium cycles and that a maximum is attained at the beginning of the large cycles.

The moving relative variation coefficient with a 3 beds window shows a clear cyclic structure of thickness variability without a linear trend. Variability is low in the sequences of beds 6-7, 14-16, 19-28a, 30-39, 42-44, 51-55, 57-62, 72-74, 81-82, and high in the sequences of beds 2-5, 11-13, 17-18, 28b-29, 40-41, 45-50, 63-65, 75-80, 83-86.

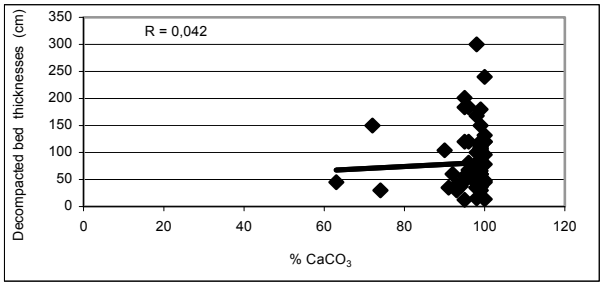

Fig. 6 – Relations between stratal patterns and lithology.

4.2. *Lithologic variations*

Relations between stratal patterns and lithology

Figure 6 relates carbonate percentage to bed thicknesses. A total independence between these 2 parameters can be observed.

5. Interpretation

5.1. *Interpretation of the stratal variation periodicity: climatic forcing by the Milankovitch orbital cycles and, by consequence, the flux of solar energy*

The previous observations enable the proposal of the following hypotheses:

- the large cycles (LC, superbundles of around 32 beds) are in relation to the 1st component of the eccentricity cycle (approximately 400 ky);
- the medium cycles (MC, bundles of approximately 8 or 9 beds, 4 MC per LC) are in relation to the 2nd component of the eccentricity cycle (approximately 100 ky);
- the small cycles (SC, with 3 to 5 beds, 2 or 3 SC per MC) record the obliquity cycles (in average 41ky);
- the very small cycles (VSC, of 2 or 3 beds) are in relation with the astronomic precession cycles (26 ky) or the climatic precession cycles (16.6 – 23 ky).

The orbital cycles

The simulation of the various orbital cycles between –132 and –128 My, using data from Berger (1978), shows the following characteristics (fig. 7):

- The large orbital eccentricity cycle (LOC, component 1) included between –130.4 and –130.0 My (fig. 7) is uncharacteristic. It comprises medium orbital cycles (MOC, component 2) that are not very clear, are of low amplitude and are not very variable. These characteristics could be at the origin of climatic and ecological modifications (crisis phenomenon) that could be related to the Hauterivian-Barremian stage boundary, which would then be positioned at –130.4 Ma (-130 ± 1,5 My according to Gradstein *et al.*, 2005). This change would be accompanied by a transgression in the Lusitanian Basin.
- On the contrary, in the –131.3_–130.3 My interval, the orbital series presents a particularly clear structure (fig. 7). In fact, it comprises 2 complete large eccentricity cycles (LOC with approximately 400 ky) and 2 incomplete ones. In the complete large cycles, three unequal high maxims (medium cycles 1 to 3), and a low maximum (medium cycle 4) correspond to the component 2 of the eccentricity cycle (MOC of approximately 100 ka). In each MOC, peaks correspond to the obliquity cycle (SOC of 41 ky) and other peaks correspond to the climatic precession cycle (VSOC of 22 ky). The time limits of the eccentricity cycles are indicated in table I. These values are approximate because of the chaotic behaviour of the solar system. However, the predictions are acceptable down to 130 My towards the past.

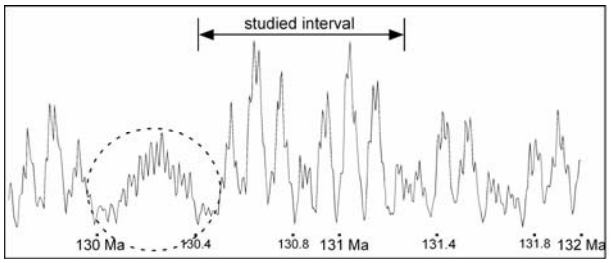

Fig. 7 – Synthetic representation (weighted sum) of the different orbital cycles between –132 and –129.6 Ma. The encircled zone corresponds to the large uncharacteristic cycle.

The visual comparison of the graphics of the orbital and thickness series (fig. 8) shows, in the -131.3_-130.3 My interval, a remarkable qualitative correspondence, both at the level of the large cycles as at the level of the

medium cycles. The abrupt increase and, after a high maximum, the slow decrease of the thickness large cycles also appear, but with less contrast, in the orbital cycles. The MOC's 2,1,3,4 are, indeed, classified in an order of decreasing amplitude.

Insolation

The combination of all orbital cycles determines the quantity of solar energy received by the Earth. By way of assumption we will admit that sedimentation mainly records not the amount of insolation but its variability (Lanci *et al*., 2010; fig. 8c). This variability probably results in an alternation of periods of climate stability and instability, and/or of periods of weak and strong seasonal contrast, influencing both the ecosystems and sedimentation. It is, in addition, very strongly correlated with the weighted sum of the orbital parameters and its graph is superimposable with that of the eccentricity.

The 400 and 100 ky eccentricity cycles are particularly clear (fig. 8c).

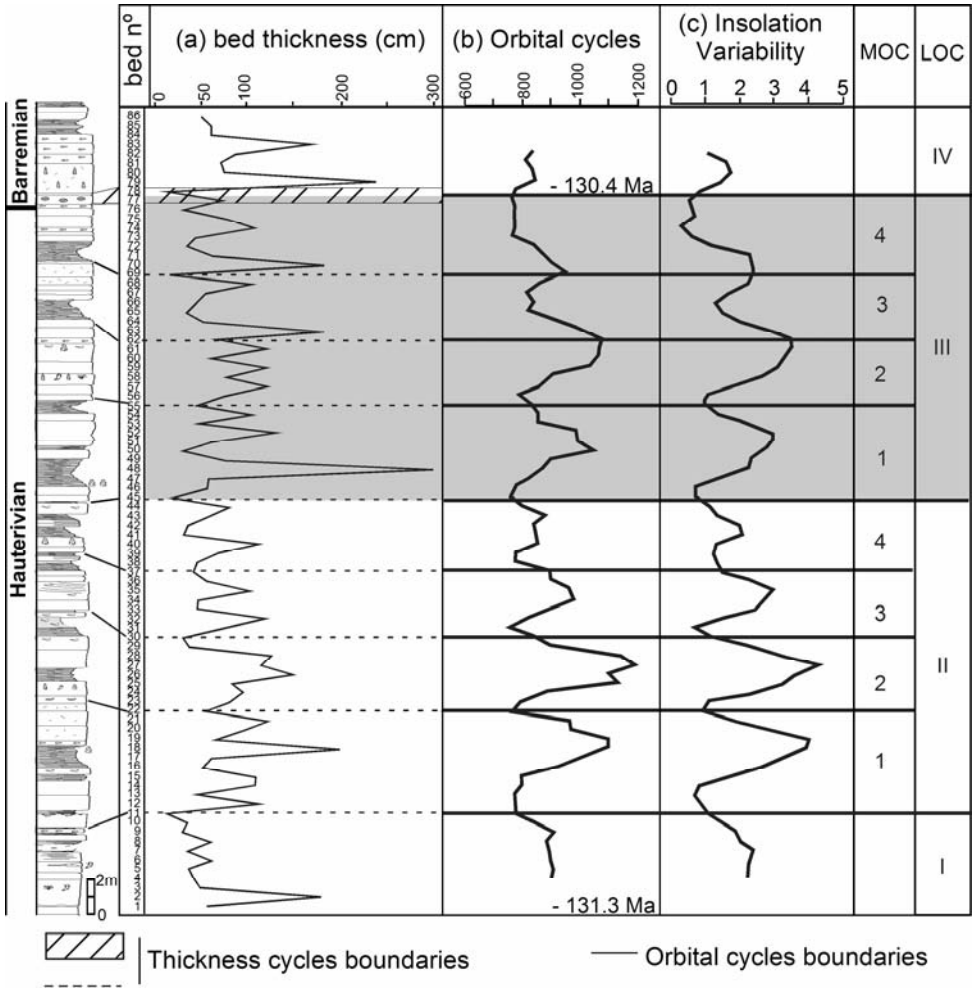

Fig. 8 – Correspondences between the thickness variation cycles and the orbital cycles.

Checking of the hypotheses

In order to check our hypotheses, we have compared the thickness series (fig. 8a) with:

– the series of combined orbital parameters (fig. 8b);
– the series of insolation variability, calculated by means of a mobile relative variation coefficient (fig. 8c).

The phase relationship between these three series is based on the correlation between the Hauterivian-Barremian boundary defined in the sedimentary series and in the astronomical series, and the estimated duration of the cycles in these three series.

In the interval of beds 11 to 79 (fig. 8), a nearly perfect superposition of the thickness and orbital parameter graphs is obtained, as well as of the thickness and insolation variability (with the condition of carrying out a slight translation in the vicinity of certain beds). It is, on the other hand, impossible to carry out a visual correspondence between the graphs in the intervals of the beds 1 to 10 and 80 to 86.

Table I proposes an estimation of the age of the cycle boundaries based on visual comparison between the astronomical series and the stratonomical series.

Large cycles (LC)	Medium cycles (MC)	Lower limit	age estimated	Number of beds
LC III - LC IV		76-78	-130400	
	MC 3 - MC 4	69	-130500	7-9
	MC 2 - MC 3	60-62	-130600	7-9
	MC 1 - MC 2	53-55	-130700	8-10
LC II - LC III		45	-130800	8-10
	MC 3 - MC 4	37	-130900	8
	MC 2 - MC 3	30	-131000	7
	MC 1 - MC 2	22	-131100	8
LC I - LC II		11	-131200	11

Tab. I – Time limits of thickness cycles and number of beds in each medium cycle.

5.2. *Identification of the cycles by spectral analysis*

After having chronologically fixed the Guincho section, we will seek, by means of spectral analysis supported on bibliographical data, the correspondence between the astronomical cycles and the stratal cycles.

Period of orbital cycles during the Hauterivian

By interpolating the graphs of Berger *et al.* (1989), one can estimate, even with low precision, the period of certain orbital cycles in the Hauterivian:

Orbital parameters	Period in ky
Obliquity 1	49.8
Obliquity 2	38.7
Average obliquity	41.0
Precession 1	22.3
Precession 2	18.3

The power spectrum of the insolation series, between -131300 and -130300 ky, lat. 30° N (128 points), has allowed to specify certain periodicities (see table below). The weighted mean period is the average of the periods included in a band, each period being weighed by its power.

Band in ky	Weighted mean period in ky	% of variance	Attribution
45.49 - 39.80	40.74	03.82	Medium obliquity
24.49 - 20.54	22.93	63.27	Precession 1
20.54 - 17.21	19.08	31.02	Precession 2

Period of thickness cycles

Figure 9 presents the spectrum of the raw data thickness series in the interval of beds 15 – 78 (64 points), theoretically corresponding to -131170 and -130410 ky; that is to say an interval of about 760 ky. The limiting-periods of each band are indicated in *number of beds* and in time (ky).

Mean period		Variance %	Attribution
number of beds	**duration in ky**		
32.0	380.0	6.1	Eccentricity 1 (LOC)
8.9	105.5	14.5	Eccentricity 2 (MOC)
4.0	48.0 Predominance of 44.7 (10.7%)	41.8	Obliquity (SOC)
2.8	32.8	13.9	?
2.2	25.9	22.8	Precession (VSOC) ?

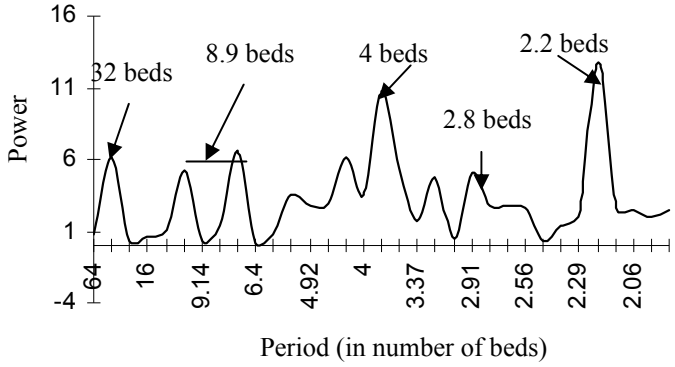

Fig. 9 – Spectral analysis of the beds thicknesses series and periodicity interpretation.

The results of the harmonic analysis complement those obtained from the morphological comparison and constitute a second checking of our hypotheses.

The correspondence between the astronomical cycles and the thickness cycles enables an evaluation of the number of beds formed during a cycle. It is however important to note that sometimes there is a relative uncertainty concerning this number (for example 7 or 8), a limit of an orbital cycle being able to be found between 2 beds:

Large orbital cycles	Medium orbital cycles	Number of beds
LOC III	MOC 4	7 - 9
	MOC 3	7 – 9
	MOC 2	10-8
	MOC 1	8-10
LOC II	MOC 4	8
	MOC 3	7
	MOC 2	8
	MOC 1	11

One should notice the decrease of the number of beds during the 4 medium cycles of a large cycle. The average number of beds is 8.5 per MOC.

6. Discussion

6.1. *Average duration of beds*

In 1994, F. Giraud indicates for the Vocontian Basin with hemipelagic sedimentation, 238 limestone-marl cycles for the Hauterivian (duration: around 5.5 My), which corresponds to approximately 23 ky for a limestone-marl cycle. Other authors indicate 21 ky. These durations are those of the climatic cycle of precession.

In the Guincho series, there are only three marly levels (< 80% of $CaCO_3$) (inner platform environment, few clastic inputs, ecosystem favouring carbonate deposition). If each limestone or argillaceous limestone bed (plus the inter-bed) represents a sedimentary cycle of 21 – 23 ky, it would be necessary to suppose, for the entire section, a duration of almost 2 My, which appears to be very excessive … unless certain beds are not grouped together.

On the other hand, it can be noticed that if one admits, by comparison with the orbital series, that the 68 beds comprised between bed numbers 11 and 78 (2 complete large cycles) cover a duration close to 800 ky, then the average duration of each one is approximately 11.8 ky, an order of magnitude of the climatic precession half-period (11.5 ky).

This duration of 800 Ky is compatible with the average duration estimated of an Hauterivian sequence (915 Ky) since, in the interval studied (beds 11 to 78), the sequence breaks up into 2 systems tracts (TST-HST), the LST missing. Thus the studied interval covers only a part of the duration of Ha7.

In each half-period of precession, the climatic contrasts are reversed from one hemisphere to another. One can make the assumption that the resulting effects (weak differences between seasons during approximately 11.5 ky – strong differences between seasons during the following 11.5 ky), although of relatively low amplitude around the 30th parallel (Dercourt *et al*., 2000), would have an affect on sedimentation. The inter-bed would coincide with this inversion. If this assumption is correct, one should find differences (geochemical or others) between 2 successive beds, formed under more or less different climatic conditions. This problem will be the subject of a later study.

6.2. *Morphological characteristics of the thicknesses graph*

Dissymmetry and homothety of the cycles

In the graphs of orbital parameters (fig. 7) calculated over long durations, large eccentricity cycles (LOC of 400 ky) are slightly dissymmetrical (amplitude of the medium cycles decreasing in the order of the cycles 2, 1, 3, 4, with a fast increase and a slower decrease; § 5.1.1). In the series of 87 bed thicknesses, the corresponding bundles (LC) are much more dissymmetrical (significantly different slopes, "saw tooth" morphology).

In certain medium cycles (MC), therefore at a different scale, one can observe a similar structure, for example in the sets 45-53, 62-69, 69-78 (fig. 4), abruptly increasing and then decreasing.

This morphology is very close to those published by several authors and concerning Quaternary 100 and 41 ky cycles (Petit *et al.*, 1999). One finds comparable figures *in* Bickert *et al.* (1997) and *in* Renard *et al.* (1997).

These cycles are characterised by an abrupt increase (steep curve, with a duration in the order of 1/5 of that of the cycle), followed by an oscillating decrease, but with a weak mean slope (duration of about 4/5 of the cycle).

In the 400 ky thickness large cycles (LC), curve morphology reproduces that of the orbital cycles and of the insolation variability, but by accentuating some contrasts.

Bi- and quadripartite structure of the cycles

Bi- and quadripartite structure of the cycles is probably in relation to the fact that the periods of the orbital cycles are close to multiples of the periods of precession (about 20 ky). One observes it in the cycles of:

- orbital parameters (400, 100, 41 and 22 ky);
- variables (proxies) regarded as influenced by the orbital parameters (Petit *et al.*, 1999, 100 ky cycles);
- Bed thicknesses (LC superbundles of 400 ky or less, divided into 4 MC bundles of 95-120 ky, each one comprising, on average, 2 SC, from 40 to 50 ky and 4 VSC, of approximately 22 ky).

Factors that control carbonate production

One of the aims of this paper was to define the major parameter which controls carbonate production in an inner platform context. By definition, this production is controlled by retroactive external and internal factors.

In this case study, the paleogeographic context (inner platform), the palaeontological associations (high density and diversity) and the scarcity of detrital contributions (see % of $CaCO_3$), tend to show that the internal parameters such as turbidity, hydro dynamism, oxygenation and salinity, play a negligible part. The temperature parameter, strongly correlated with the climatic factor, seems to have a major influence.

The climate evolution – thus the temperature evolution – will influence the growth potential of the platforms while acting directly on the development of the producing carbonate organisms and also on their activity.

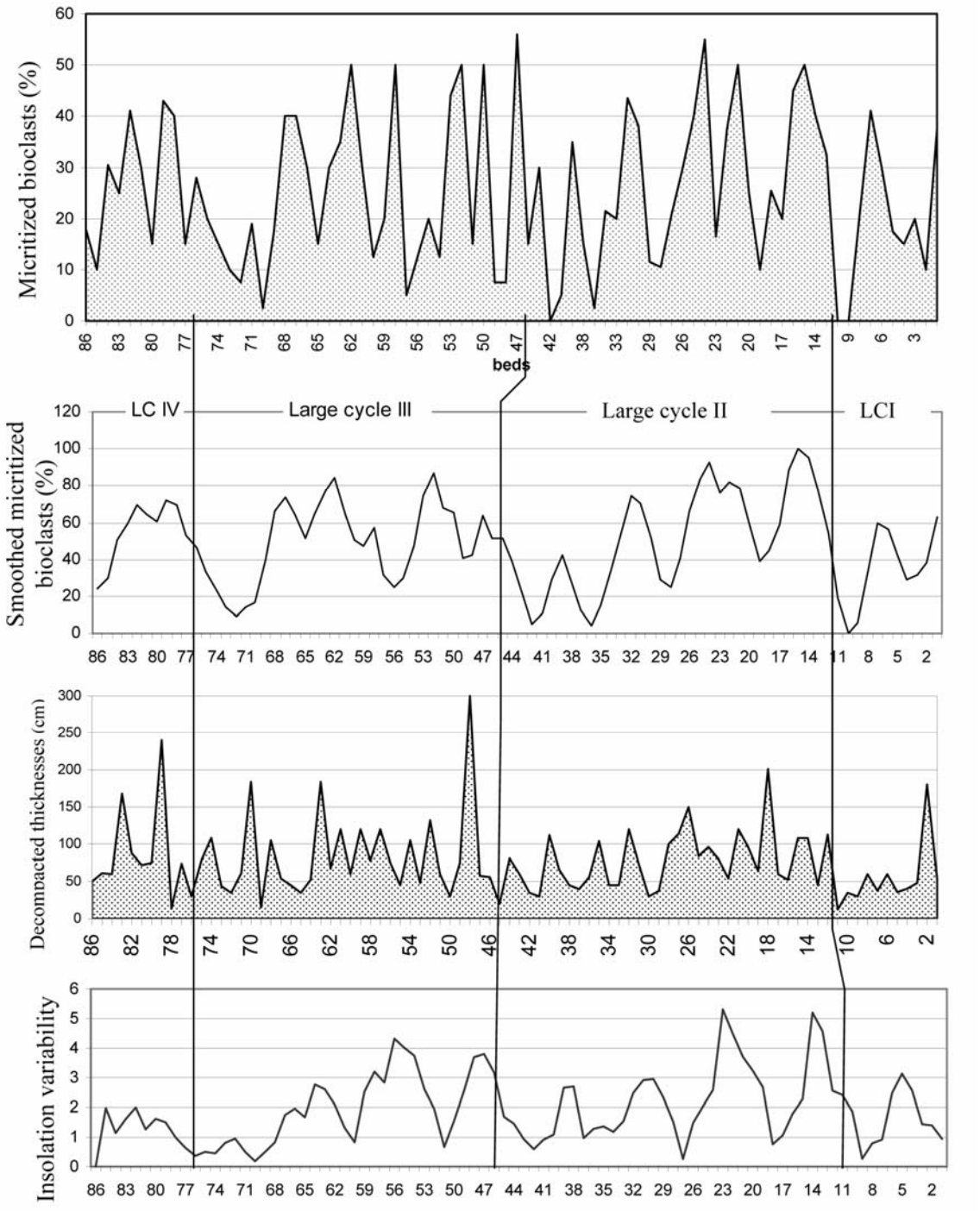

Fig. 10 – Correspondences between the insolation variability, the stratal thickness variation and the micritized bioclasts concentration variation.

In the studied series, the producers are benthic Foraminifera, gastropods (Nerinae, Naticid and *Ptygmatis* sp.), lamellibranchiata (*Exogyra tuberculifera*), Echinodermata and calcareous algae. The rudists and the corals contribution, because of their rare occurrence and their reworking, remain negligible. Micritization is intense, inducing a mechanical and diagenetic synsedimentary modification of all types of grains. This complex process testifies the activity of perforating and micritizing organisms (microplants, fungus, bacteria). Presently, it works under certain palaeoenvironmental conditions, such as shallow, clear and warm waters, with moderate hydrodynamism. The micritized elements abound between 0 and 10 m of depth, in the photic zone (Purser, 1980).

The organic activity can thus be estimated from the quantification of the micritized elements (fig. 10). The biological contents in Guincho section (see § 2.1) suggest that the conditions supporting micritization were present in the sedimentary environment. The curve of the values of the concentration in micritized elements shows a very clear cyclicity. The determination of the autocorrelation coefficient and the spectral analysis (fig. 11) reveal that this cyclicity presents the same periodicity as the bed thicknesses variation and, consequently, as the orbital series. The periodicity is, in particular, the same as the first and second component of the eccentricity, which suggests a climatic influence on the presence and activity of the micritizing and perforating organisms.

Mean period		**Variance %**	**Attribution**
Band: *number of beds*	**Band: duration in ky**		
32	380.0	8.3	Eccentricity 1 (LOC)
16	190.0	6.7	Harmonic of Eccentricity
9.1	108.0	14.7	Eccentricity 2 (MOC)
6.3	74.0	18.2	?
4.2	49.0	15.0	Obliquity (SOC)
2.8	34	26.4	Precession (VSOC) ?
2.1	25	2.5	Precession (VSOC) ?

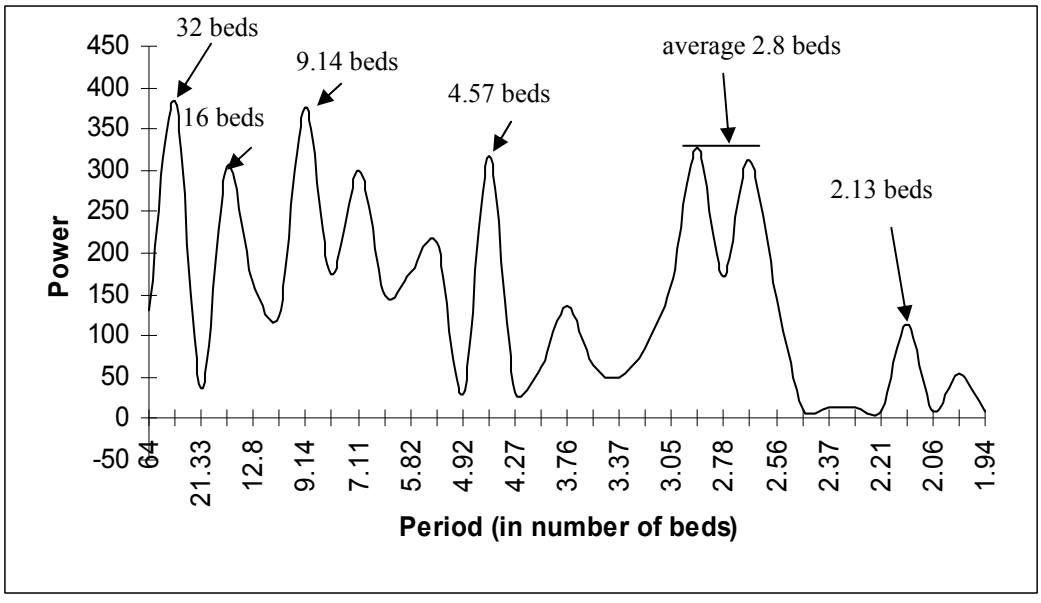

Fig. 11 – Spectral analysis of the micritized bioclasts series and periodicity interpretation.

This interpretation is confirmed by the good visual correspondence between the curve of the insolation variability and the curve of the concentration values in micritized elements (fig. 10), and by the high value of the linear correlation coefficient between these 2 series ($R = 0.54$, $p < 0.01\%$, with a delay of 3 beds between micritization and insolation; $R = 0.47$, $p < 0.01\%$, with a delay of 2 beds; $R = 0.54$, $p = 0.54\%$, with a delay of 1 bed).

The intense micritization at the beginning of a large cycle would be related to strong insolation variability and a deceleration of this process at the end of the cycle associated to low insolation variability.

The climate impact on this process of micritization is in total agreement with the observations carried out in the quaternary series (Purser, 1980).

In view of these various results, climatic control on quantitative and qualitative carbonate production seems to be undeniable. In inner platform environments higher insolation variability would engender both higher carbonate production and higher sedimentation rates.

7. Conclusions

The study of the stratal, biofacies and lithofacies variations found at the top of the late-Hauterivian series (sequence Ha7) that outcrops at Guincho (Portugal) has lead to the following results:

a) The bed thickness series comprises 2 composite large cycles preceded and followed by incomplete large cycles.

b) The graphs of the thickness cycles are comparable to those of the combined orbital cycles and the insolation variability.

From this observation, we conclude that, in an inner platform environment with continuous carbonate sedimentation in an aggradational context, the stratal variations, reflecting the fluctuations of the carbonate production rate, are controlled by orbital parameters.

Four major orders of periodicity were detected in the Guincho section:

- Large Cycles (LC superbundles of 31-32 beds), recording the component 1 of the 400 ky eccentricity cycle (LOC);
- Medium Cycles (MC bundles of about 8 or 9 beds), in connection with the component 2 of the 95-120 ky eccentricity cycle (MOC);
- Small Cycles (SM of 4-5 beds), recording components 1 and 2 (49 and 39 ky, in the Hauterivian) of the obliquity cycle (SOC);
- Very Small Cycles (VSC of 2-3 beds), in connection with components 1 and 2 (26 and 22-23 ky) of the precession (VSOC).

These cycles affect both argillaceous limestones and limestones indifferently.

Orbital forcing, an external phenomenon, appears to be the major factor. However, the thickness cycles are less regular than the orbital cycles. These irregularities may be due to:

- the influence of other cycles, planetary or not;
- the non-linearity of the responses to insolation;
- random or chaotic phenomena characteristic of the Earth system (randomness of sedimentation rates, bioturbation, sampling problems …);
- internal forcing: interactions, feedback between sub-systems (climate, vegetation, plankton, biosphere in general, atmospheric and oceanic circulations);
- local phenomena.

To consider insolation as the only influence is a reductionistic attitude. As in all natural systems, we are in the presence of multiple factor phenomena.

c) The average duration of a bed is approximately 11.8 ky. This duration can be brought back to 11.5 ky, a value equal to that of the hemi-cycle of precession, if it is supposed that 4 beds are missing between levels 11 and 77. The sedimentary cycle (22-23 ky) would be of argillaceous limestones only instead of marl-limestones characteristic of deep environments. The interbed would correspond to the climatic inversion between the 2 hemi-cycles.

d) Climatic control on quantitative and qualitative carbonate production is confirmed by the close relation between the bed thicknesses variations, the insolation variability and the micritized elements concentration variations. The percentage in these last elements increases at the beginning of cycle when the bed thickness is most important and the insolation variability is the strongest. At the end of the cycle these three parameters reach minimal values.

In addition, the curve of the values of the concentration in micritized elements has a cyclic structure at various scales whose periodicities are close, or identical, to the stratonomic and thus orbital periodicities.

References

ARNAUD-VANNEAU A. (1980) – Micropaléontologie, paléoécologie et sédimentologie d'une plate-forme carbonatée de la marge passive de la Téthys. L'Urgonien du Vercors septentrional et de la Chartreuse (Alpes occidentales). *Géol. Alpine* Mém. Sp. 11 (3), 874 p.

ARNAUD-VANNEAU A. & DARSAC C. (1984) – Caractère et évolution des peuplements de foraminifères benthiques dans les principaux biotopes des plates-formes carbonatées du Crétacé inférieur des Alpes du Nord (France). *Géobios* Mém. Sp. 8, 19-23.

BERGER A. L. (1978) – Long-term variations of daily insolation and Quaternary climatic changes. *Journal Atmospheric Sciences* 35, 2362-2367.

BERGER A. L., LOUTRE M. F. & DEHANT V. (1989) – Astronomical frequencies for pre-Quaternary palaeoclimate studies. *Terra Nova* 1, 474-479.

BICKERT T., CURRY W. B. & WEFER G. (1997) – Late Pliocene to Holocene benthic stable isotopes. *Proceed. Ocean Drilling Program, Scientific Results* 154, 239-254.

CHATFIELD C. (1975) – *The Analysis of Time Series, Theory and Practice*. Chapman & Hall, London, 263 p.

CUGNY P. (1988) – Modèles paléoécologiques. Analyse quantitative des faciès dans diverses formations crétacées des marges néotéthysiennes et atlantiques, associations paléontologiques et paléoenvironnementales. *Strata* 2 (10), 331 p.

D'ARGENIO B., FERRERI V., AMODIO S. & PELOSI N. (1997) – Hierarchy of high-frequency orbital cycles in Cretaceous carbonate platform strata. *Sedimentary Geology* 113, 169-193.

DERCOURT J., GAETANI M., VRIELYNCK B., BARRIER E., BIJU-DUVAL B., BRUNET M. F., CADET J. P., CRASQUIN S. & SANDULESCU M. (2000) – *Atlas Peri-Tethys, Palaeogeographical Maps*. CCGM/CGMW, Paris, 24 maps, explanatory notes I-XX: 269 p.

FISCHER A. G. & SCHWARZACHER W. (1984) – Cretaceous bedding rhythms under orbital control? *In*: BERGER A. *et al.* (Édit.), *Milankovitch and climate*, part I, 163-175.

FOUCAULT A. & RENARD M. (1987) – Contrôle climatique de la sédimentation marno-calcaire dans le Mésozoïque d'Espagne (Sierra de Fontcalent, province d'Alicante): arguments isotopiques. *C. R. Ac. Sci. Paris* 305, sér. II, 517-521.

FLÜGEL (2004) **–** *Microfacies of Carbonate Rocks. Analysis, Interpretation and Application*. Springer-Verlag, Berlin, 976 p.

GIRAUD F. (1994) – *Recherche des périodicités astronomiques et des fluctuations du niveau marin à partir de l'étude du signal carbonate des séries pélagiques alternantes. Application au Crétacé inférieur du Sud Est de la France, de l'Atlantique central et du golfe du Mexique*. Thèse Univ. Claude Bernard, Lyon I (unpublished), 239 p.

GRADSTEIN F. M., OGG J. G. & SMITH A. G. (2005) – *A Geologic Time Scale 2004*. Cambridge University Press, 589 p.

HARDENBOL J., THIERRY J., FARLEY M. B., JACQUIN TH., GRACIANSKY P. C. DE & VAIL P. R. (1998) – Mesozoic and Cenozoic Sequence Chronostratigraphy Framework of European Basins. *In*: GRACIANSKY P. C. DE, HARDENBOL J., JACQUIN TH. & VAIL P. R. (Eds.), *Mesozoic and Cenozoic Sequence Stratigraphy of European Basins*, SEPM Sp. Publ., Tulsa, 60.

HILLGÄRTNER H. & STRASSER A. (2003) – Quantification of high-frequency sea-level fluctuations in shallow-water carbonates: an example from the Berriasian-Valanginian (French Jura). *Palaeogeogr., Palaeoclim., Palaeoecol.* 200, 43-63.

HUFTY A. (2001) – *Introduction à la climatologie*. De Boeck Univ. & Presses Univ. Laval, 544 p.

JOHNSON M. M. (1972) – A test for periodic effects in time series data. *Int. J. Systems Sci.* 3 (1), 85-92.

KENNETT J. P. (1982) – *Marine Geology*. Prentice-Hall, Englewood Cliffs, New Jersey, 813 p.

LANCI L., MUTTONI G. & ERBA E. (2010) – Astronomical tuning of the Cenomanian Scaglia Bianca Formation at Furlo, Italy. *Earth Planetary Sci. Letters* 292, 231-237.

PETIT J. R., JOUZEL J., RAYNAUD D., BARKOV N. I., BARNOLA J.-M., BASILE I., BENDERS M., CHAPPELAZ J., DAVIS M., DELAYGUE G., DELMOTTE M., KOTLKYAKOV V. M., LEGRAND M., LIPENKOV V. Y., LORIUS C., PÉPIN L., RITZ C., SALTZMAN E. & STIEVENARD M. (1999) – Climate and atmospheric history of the past 420 000 years from the Vostok ice core, Antarctica. *Nature* 399, 429-436.

PURSER B. H. (1980) – *Sédimentation et diagenèse des carbonates néritiques récents*. Technip Éd., Paris, tome 1, 366 p.

RENARD M. (Coord.), DAUX V., CORBIN J.-C., EMMANUEL L. & BAUDIN F. (1997) – La chimiostratigraphie. *In*: REY J. (Coord.), *Stratigraphie. Terminologie française*. Bull. Centres Rech. Explor.-Prod. Elf Aquitaine Mem. 19, 37-50.

REY J. (1972) – Recherches géologiques sur le Crétacé inférieur de l'Estremadura. *Mem. Serv. Geol. Portugal* N.S. 21, 477 p.

REY J. & CUGNY P. (1977) – Ecoséquences et paléoenvironnements de l'Albien du Portugal. *Bull. Soc. Hist. Nat. Toulouse* 113, 374-386.

REY J., GRACIANSKY P. C. DE & JACQUIN TH. (2003) - Les séquences de dépôt dans le Crétacé inférieur du Bassin Lusitanien. *Comun. Inst. Geol. Min*. 90, 15-42.

STRASSER A., PITTET B., HILLGÄRTNER H. & PASQUIER J.-B. (1999) – Depositional sequences in shallow carbonate-dominated sedimentary systems: concepts for a high-resolution analysis. *Sedimentary Geology* 128, 201-221.

TRICOT C. H. & BERGER A. (1988) – Long and short term variability of climate. *In*: WANNER H. & SIEGENTHALER U. (Eds.), *Sensibility of present-day climate to astronomical forcing*. Springer-Verlag, Berlin, 135-152.

VILLIER L. (2001) – *Evolution du genre* Heteraster *dans le contexte de radiation de l'ordre des Spatangoida (Echinoidea, Echinodermata) au Crétacé inférieur*. Thèse Univ. Bourgogne, Dijon, 248 p.

YANG W. & LEHRMANN D. J. (2003) – Milankovitch climatic signals in Lower Triassic (Olenekian) peritidal carbonate successions, Nanpanjiang Basin, South China. *Palaeogeogr., Palaeoclim., Palaeoecol.* 201 (3-4), 283-306.

ZHANG K. – J., XIA B. & LIANG X. (2002) – Mesozoic-Paleogene sedimentary facies and paleogeography of Tibet, Western China: tectonic implications. *Geological Journal* 37, 217-246.